AJNR

Multi-Detector Row CT Angiography in the Assessment of Carotid Artery Disease in Symptomatic Patients: Comparison with Rotational Angiography and Digital Subtraction Angiography

Marja Berg, Zishu Zhang, Aki Ikonen, Petri Sipola, Reetta Kälviäinen, Hannu Manninen and Ritva Vanninen

AJNR Am J Neuroradiol 2005, 26 (5) 1022-1034
http://www.ajnr.org/content/26/5/1022

Multi-Detector Row CT Angiography in the Assessment of Carotid Artery Disease in Symptomatic Patients: Comparison with Rotational Angiography and Digital Subtraction Angiography

Marja Berg, Zishu Zhang, Aki Ikonen, Petri Sipola, Reetta Kälviäinen, Hannu Manninen, and Ritva Vanninen

BACKGROUND AND PURPOSE: **Compared with the single-detector technique, multi-detector row CT angiography permits larger anatomic coverage that includes both the epiaortic and entire carotid circulations. We evaluated the accuracy of multi-detector row CT angiography by using multiplanar reformation (MPR) for measuring carotid artery diameters compared with that of rotational angiography. We also evaluated the diagnostic performance of CT angiography compared with digital subtraction angiography (DSA).**

METHODS: **In 35 patients, CT angiograms of 70 carotid arteries were compared with DSA images, and CT angiograms of 33 carotid arteries were compared with rotational angiograms. CT angiographic interpretation was performed first interactively at a workstation. Diameter measurements of normal and stenosed carotid arteries were performed on cross-sectional and oblique sagittal MPRs. Degree of stenosis was calculated per North American Symptomatic Carotid Endarterectomy Trial criteria independently by two observers for each technique.**

RESULTS: **Degree of stenosis was slightly underestimated with CT angiography, with mean differences (± SD) per observer of 6.9 ± 17.6% and 10.7 ± 16.1% for cross-sectional and 2.8 ± 19.2% and 9.1 ± 16.8% for oblique sagittal MPRs compared with rotational angiography. CT angiography was somewhat inaccurate for measuring the absolute minimal diameter of high-grade stenoses. On symptomatic sides (n = 35), interactive CT angiographic interpretation combined with MPR measurements for lesions with a visual estimate of 50% or greater stenosis achieved a sensitivity of 95% (20/21) and specificity of 93% (13/14) in the detection of carotid stenosis (≥ 50%) verified with DSA.**

CONCLUSION: **Regardless of slight underestimation of carotid stenosis with CT angiography compared with rotational angiography, diagnostic performance of CT angiography with interactive interpretation proved to be good. Also, the method is highly sensitive for detection of carotid artery stenosis, indicating the suitability of CT angiography as a screening method for symptomatic patients. For hemodynamically significant stenoses revealed by CT angiographic screening, conventional angiography still seems to be necessary.**

CT angiography is a useful tool for evaluation of cerebrovascular vessels. New multi-detector row CT technology provides several advantages for carotid imaging in comparison with the single-detector technique (1). Multi-detector row CT angiography permits larger anatomic coverage, including both the epiaortic and entire carotid circulation with the branches of the circle of Willis (2). Multi-detector row

Received June 24, 2004; accepted after revision September 21.

From the Departments of Clinical Radiology (M.B., Z.Z., A.I., P.S., H.M., R.V.) and Neurology (R.K.), Kuopio University Hospital, Finland; and the Department of Radiology, 2nd Hospital of Xiangya Medical School, Central South University, Changsha, Peoples Republic of China (Z.Z.)

Supported by grants from the Radiological Society of Finland, the Finnish Cultural Foundation, and Kuopio University Hospital grant no. 5063501.

Presented in part at the 16th European Congress of Radiology, Vienna, Austria, March 7–11, 2003.

Address correspondence to Marja Berg, MD, Department of Clinical Radiology, Kuopio University Hospital, Puijonlaaksontie 2, Fin-70210 Kuopio, Finland.

CT has been proposed to be useful in the comprehensive imaging of ischemic stroke (3). To our knowledge, no previous studies have considered the diagnostic performance of multi-detector row CT angiography for the assessment of carotid artery stenosis.

Rotational angiography with multiple projections may provide benefit over digital subtraction angiography (DSA) in determining the smallest diameter in a stenosed carotid artery (4, 5). CT angiography is a true cross-sectional imaging method. To evaluate the accuracy of CT angiography in measuring diameters in practice, the best reference method available should be used. To our knowledge, there are no published studies in which CT angiography has been compared with rotational angiography for the assessment of carotid diameters. However, DSA is still the current reference standard for clinical decision-making.

The purpose of the present study was to assess the accuracy of multi-detector row CT angiography in the assessment of carotid artery diameters compared with that of rotational angiography and to assess the diagnostic performance of CT angiography for detection of carotid stenosis compared with DSA.

Methods

Study Protocol and Patients

Between September 2001 and June 2002, all patients who were scheduled for DSA of the cervicocranial arteries because of transient ischemic attacks or minor hemispheric stroke and who had normal renal function were asked to participate in the study. Thirty-five consecutive patients (20 men, 15 women; mean age, 68 years; range, 50–83 years) participated the study. Both DSA and CT angiography were performed during the inpatient time. The study protocol was approved by the ethics committee of our hospital, and informed consent was obtained from the patients.

Angiography

Selective angiography was performed for 70 carotid arteries in 35 patients by using biplane DSA equipment (Neurostar Plus; Siemens, Forchheim, Germany). Each carotid artery was imaged in four projections with 5–6 mL of nonionic contrast medium (Visipaque 270 mg of iodine/mL; Nycomed, Oslo, Norway) per injection and a flow rate of 8 mL/s. The four projections used in DSA were anteroposterior, lateral, ipsilateral oblique, and contralateral oblique projections obtained in both carotid arteries. In addition, the aortic arch and subclavian arteries were imaged.

Rotational angiography was performed if the radiologist anticipated that the patient was capable of staying motionless for the approximately 24 seconds necessary to complete the entire rotational angiographic imaging protocol, including imaging with nonenhanced and enhanced projections and a minor pause before these two rotations. The patient was positioned in the isocenter of the equipment. For enhanced rotational imaging, 23 mL of contrast medium was injected at a flow rate of 2.5 mL/s into the common carotid artery. After contrast medium injection, imaging started in a lateral position with 180° rotation in 8 seconds around the carotid bifurcation to acquire 80 projections. A 512 × 512 image intensifier matrix was used. Rotational angiography was performed in a total of 33 bifurcations (one carotid bifurcation for 29 patients, both carotid bifurcations for two patients). For statistical purposes, rotational angiography was performed randomly on either the symptomatic or contralateral side or both sides to gather a wide range of stenoses.

Evaluation of DSA and Rotational Angiography

The DSA and rotational angiographic images were analyzed by using the routine console of the angiography equipment. For rotational angiography, the site of maximal stenosis was evaluated by using the acquired 80 original angiograms. The stenosis percentage was measured by using the criteria described by the North American Symptomatic Carotid Endarterectomy Trial (NASCET) Collaborators (6). For windowing of DSA images, the observer was allowed to change the settings on a visual basis as usual in daily practice.

In rotational angiography, the windowing of the original nonsubtracted projections was selected by the observer to show enhanced vessels properly with sufficient contrast in relation to the background. Two radiologists (Z.Z., A.I.) with 9 and 5 years experience for performing and interpreting carotid angiographic studies independently measured the minimum diameter at the stenosis level from the projection showing maximum stenosis in the internal carotid artery (ICA), or the common carotid artery (CCA) if this was of greater severity. The reference diameter was set distal to the carotid bulb. The measured stenosis degrees were classified into five categories: 0–29%, 30–49%, 50–69%, 70–99%, and occlusion of the carotid artery.

Ulcerations of the plaques, distal carotid artery lesions (beyond the bulb), and additional findings such as intracranial aneurysms were also recorded. Distal carotid artery stenosis was measured, and the ratio of the degree of stenosis was defined by using the diameter of the normal artery in the same segment as the reference.

CT Angiography

All patients underwent CT angiography with a four-channel multi-detector row CT system (Volume Zoom; Siemens). The scanning was performed with 120 kV and 250 mAs. The other imaging parameters were 1-mm collimation, 5-mm/s table feed, and 0.5-second gantry rotation time. The contrast agent (Ultravist 300 mg of iodine/mL; Schering AG, Berlin, Germany) volume for CT angiography was 80 mL, with a saline chaser bolus of 30 mL by using a flow rate of 3 mL/s with a 1.3-mm (18 gauge) cannula through the antecubital vein. The bolus-tracking method was used for assessment of the optimal time delay for CT scanning, to optimize contrast material enhancement in carotid arteries; the region-of-interest indicator was placed on a reference image obtained from the aorta. Scanning started 5 seconds after enhancement in the aorta reached 70 HU. Spiral scanning included the volume between the sixth cervical vertebra and the circle of Willis. The patients were asked to breathe evenly and smoothly without swallowing or moving. The raw data of CT angiography were routinely reconstructed to axial sections with a soft-tissue algorithm and a section thickness of 1.5 mm with a 1.0-mm reconstruction interval.

Evaluation of CT Angiograms

The axial images were loaded on a separate workstation (ADW 4.0; GE Medical Systems, Milwaukee, WI) for further analysis. A window width of 700 and window level of 200 were selected for the interactive interpretation of the carotid CT angiographic study and for the subsequent multiplanar reformation (MPR) measurements. Three radiologists (M.B., Z.Z., P.S.) analyzed the CT angiographic data independently. The observers first viewed the bifurcation area of both carotid arteries interactively at the workstation to obtain a general overview of the vessels and to detect the possible sites of

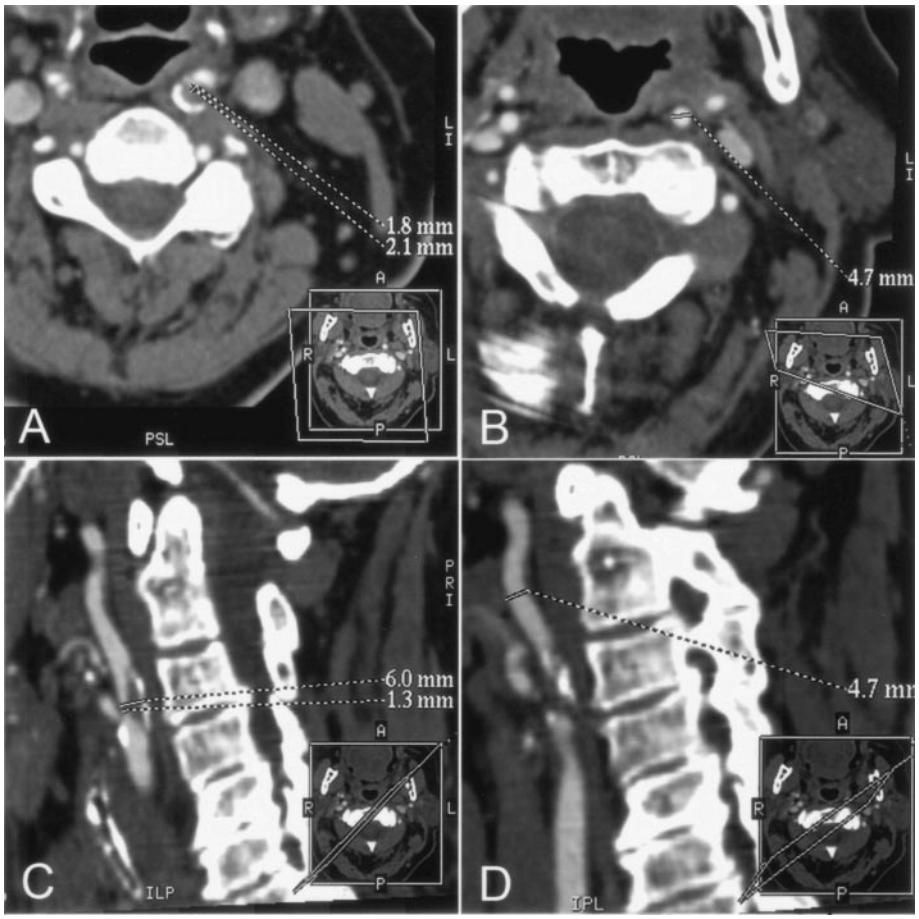

FIG 1. *A–D*, CT angiographic MPR images of the left ICA at the stenosis level (*A* and *C*) and at the distal extracranial ICA as the chosen reference level (*B* and *D*) for assessment of stenosis degree with NASCET criteria. Dotted lines indicate sites of measurement of vessel diameter. Every view was tilted according to the patient's individual anatomy; the tilted planes are shown in small boxes in the right lower corner of each image.

A and *B*, Cross-sectional MPR images (data were reformatted with the double oblique mode) illustrate the accurate cross-section of the artery at the stenosis level (*A*) and at the chosen reference level (*B*). At the stenosis level, the minimum diameter was determined with an additional measurement perpendicular to the smallest diameter.

C and *D*, Oblique sagittal MPR images tilted along the course of the obliquely oriented ICA at the level of stenosis (*C*) and at the chosen reference level in the distal extracranial ICA (*D*) . At the stenosis level, the actual diameter of the entire ICA (upper dotted line in *C*), including the patent vessel lumen and the plaque, is shown.

stenosis and additional findings. A filling pouch of contrast medium within the plaque was interpreted as ulceration.

The distal cervical and intracranial parts of the ICA were evaluated by one of the observers with 8 years experience in performing CT angiography, in the cine mode in three orthogonal planes for detection of significant distal stenosis above the bifurcation as a possible tandem lesion and also for detection of other findings.

For the assessment of the degree of stenosis, the oblique cross-sectional MPR and oblique sagittal MPR, which are perpendicular to each other, were reconstructed by each observer. Figures 1 and 2 show examples of these 2D MPR subvolume images. Although analysis of axial images reveals the contrast-enhanced lumen whether or not there are mural calcifications, an axial image of the stenosed carotid artery deflecting from the scanning plane may fail to reveal exactly the shortest diameter of the stenosed segment (Fig 2). Therefore, the stenosis degree was measured from the MPR views, and two observers (M.B., Z.Z.) independently measured the diameter stenosis degree by using the NASCET criteria. To assess intraobserver repeatability, one observer without previous experience in performing CT angiography analyzed the data twice with an interval of 1 month. One observer (P.S.) with 1 year of experience in performing CT angiography did only interactive visual interpretation of the CT angiographic study and estimated the degree of the stenosis.

The measurements were performed from magnified MPR images with an electronic caliper at the workstation. In cases of a string sign, the diameter stenosis degree was interpreted to be 95%, similarly as in previous angiographic studies (7). Finally, the visual estimation of stenosis degree was combined with MPR measurements for selected cases as a two-step procedure (i.e., interactive interpretation of CT angiograms with subsequent MPR measurements).

Statistical Analysis

All data were analyzed with the SPSS 10.1 for Windows (SPSS Inc., Chicago, IL) statistical package. The Pearson correlation coefficient was calculated to assess the intraobserver reproducibility and the interobserver agreement. The κ statistic was calculated for the interobserver agreement of CT angiographic measurements and for the intertechnique comparison. Linear regression analysis with a standard error of estimation (SEE) was used for the assessment of intra- and interobserver error between hemodynamically insignificant ($<50\%$) and significant ($\geq 50\%$) stenoses, divided according to the findings at rotational angiography. Mean difference with SD was calculated for the interobserver agreement of rotational angiography measurements and for the intertechnique comparison. Scatterplots were constructed for the intertechnique comparison of the absolute diameter measurements. Differences for continuous variables with a normal distribution were analyzed with the *t* test for paired observations. A *P* value of less than .05 was considered to indicate a statistically significant difference. To assess the diagnostic performance of CT angiography, sensitivity, specificity, and overall accuracy values were calculated by using 50% diameter stenosis as the cutoff point for a hemodynamically significant finding. The diagnostic performance with positive and negative predictive values was also calculated separately for the symptomatic side.

Results

DSA and Rotational Angiography

Among the 70 carotid arteries analyzed, there were 27 grade 0–29% stenoses, 13 grade 30–49% stenoses,

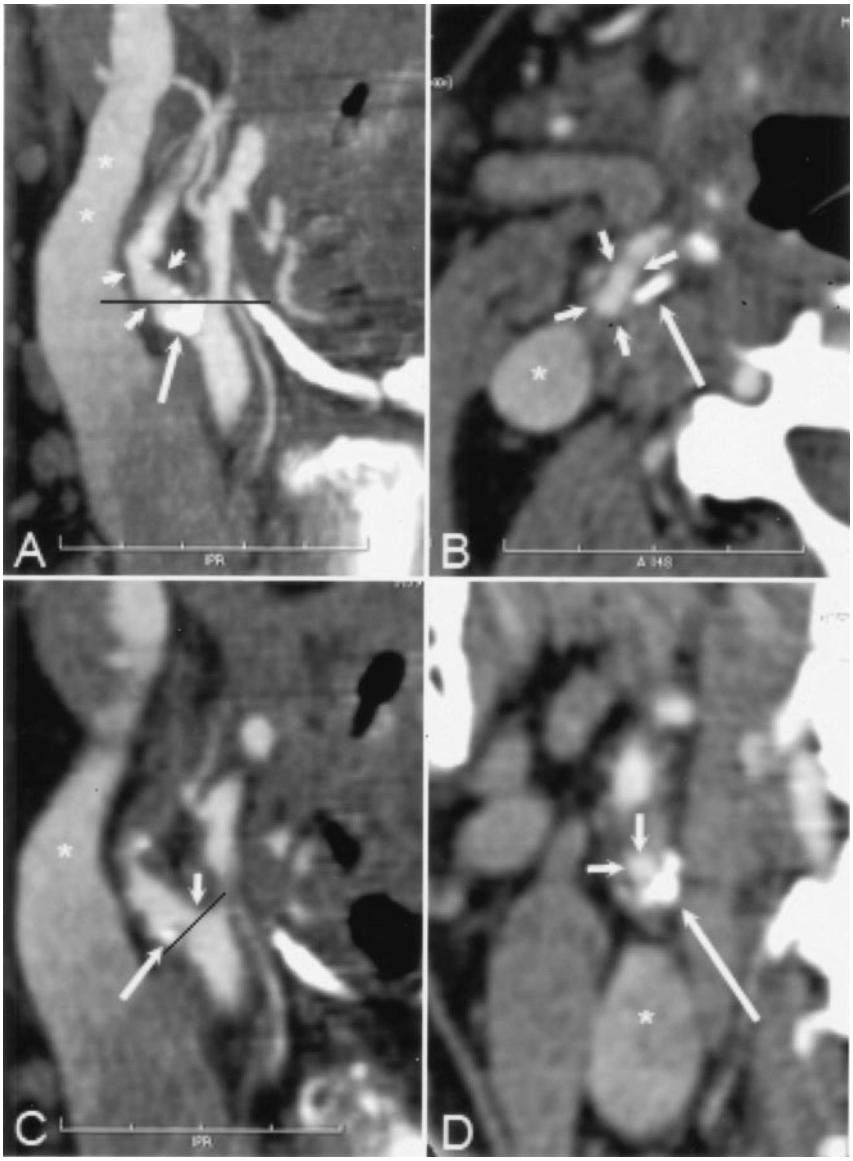

FIG 2. *A* and *B*, CT angiographic thin-slab MIP images with slab thickness of 6 mm in the right carotid artery reveals atherosclerotic changes (short arrows in *A*) and an extensive mural calcification (long arrow in *A* and *B*) in the bulbar area of the ICA. The black line in *A* indicates the corresponding axial plane in *B*. Note that the course of the ICA seen entirely on the MIP image deflects from the caudocranial scanning plane. Therefore, the cross-section of the ICA (short arrows in *B*) is elongated. Asterisk indicates partly enhanced jugular vein.

C, Oblique sagittal MPR image with section thickness of 0.3 mm shows that the hemodynamically insignificant stenosis (short arrow) is seen next to the mural calcification (long arrow), which hides the stenosis area seen on the MIP image in *A*. Black line indicates the orientation of the cross-sectional MPR image in *D*; asterisk indicates partly enhanced jugular vein.

D, Cross-sectional MRP image shows a concentric plaque in the ICA wall with eccentrically located extensive mural calcification (long arrow), and the enhanced lumen (short arrows) appears circular. Asterisk indicates partly enhanced jugular vein. According to our experience, it was slightly easier to determine the maximal stenosis point of the carotid artery with cross-sectional MPR than with sagittal MPR mode. With sagittal MPR mode, it is possible to rotate the image plane 360°, leading to inaccuracy in detecting the shortest diameter in eccentric stenoses. In addition, during the procedure to produce the MPR images at the GE workstation, there is a mark point on the target vessel (not shown) that sometimes hampers visualization of the stenosed carotid artery, especially with sagittal MPR mode.

eight grade 50–69% stenoses, 17 grade 70–99% stenoses, and five occlusions on DSA images. DSA enabled detection of 25 stenoses with an ulceration. Nine distal lesions in the intracranial ICA were verified on DSA images among the 65 patent distal carotid arteries (Fig 3). In addition, one occult intracranial aneurysm was detected. On the symptomatic side (n = 35), the mean stenosis was 57% with DSA (range, 0–100%). The carotid stenoses on the symptomatic side of the patients were hemodynamically significant (≥ 50%) in 21 patients and hemodynamically insignificant in 14 patients.

According to rotational angiography (n = 33), there were 10 grade 0–29% stenoses, six grade 30–49% stenoses, eight grade 50–69% stenoses, eight grade 70–99% stenoses, and one occlusion. Rotational angiography was performed on the symptomatic side in 16 patients. On rotational angiograms, the mean smallest diameter (± SD) of the absolute residual lumen was 4.6 ± 0.8 mm (range, 3.6–6.2 mm, n = 10) in the category of 0–29% stenosis, 2.5 ± 0.5 mm (range, 2.1–3.2 mm, n = 6) in the category of 30–49% stenosis, 1.6 ± 0.4 mm (range, 1.1–2.0 mm, n = 8) in the category of 50–69% stenosis, and 1.0 ± 0.2 mm (range, 0.8–1.2, n = 8) in the category of 70–99% stenosis.

The mean difference between measurements from DSA and rotational angiography was –2.3 ± 9.1% (P = .155), indicating a slight underestimation with DSA compared with rotational angiography. Table 1 shows the comparison of DSA with rotational angiography. In one carotid artery, the string sign was detected with DSA; rotational angiography was not performed in this case.

An excellent correlation was demonstrated between the two observers for the measurements with DSA (r = 0.95, $P < .001$, n = 70) and rotational angiography (r = 0.95, $P < .001$, n = 33). The mean difference (± SD) between observers was 0.5 ± 10.6% with DSA and 0.3 ± 9.5% with rotational angiography.

FIG 3. Distal lesion in the petrous part of the left ICA detected correctly with CT angiography.

A and *B*, Axial (*A*) and coronal (*B*) MPR images of distal ICAs show the smaller diameter of the left ICA (long arrow) compared with the normal ICA on the right (short arrow).

C and *D*, Selective angiograms verify the stenosis (arrow in *C*) and a near-occlusion (arrow in *D*) at the bulb. This tandem lesion on the symptomatic side was successfully treated with angioplasty and stent placement.

TABLE 1: Comparison of stenosis grade at DSA and rotational angiography in 33 arteries

	Rotational Angiography					
DSA	0–29%	30–49%	50–69%	70–99%	100%	
0–29%	10	1				11
30–49%		4	3			7
50–69%		1	4			5
70–99%			1	8		9
100%					1	1
	10	6	8	8	1	33

Note.—Data are number of arteries in which both DSA and rotational angiography were performed.

Reproducibility of CT Angiographic Measurements

The Pearson correlation coefficient (r) between the repeated stenosis degree measurements for a single observer (n = 70) was 0.79 ($P < .001$) by using cross-sectional MPR and 0.77 ($P < .001$) by using oblique sagittal MPR. The correlation between the two observers was 0.83 ($P < .000$) for the cross-sectional MPR measurements and 0.77 ($P < .001$) for the oblique sagittal MPR measurements.

Fair to moderate agreement was detected between the two observers at the cutoff point of 50% stenosis degree, achieving a κ statistic value of 0.52 (95% confidence interval [CI]: 0.32–0.72) for cross-sectional MPR and 0.49 (95% CI 0.30–0.69) for oblique sagittal MPR.

For measuring the degree of stenosis with cross-sectional MPR, the intra- and interobserver error expressed as the SEE was of the same order for both hemodynamically insignificant and significant stenoses. For insignificant stenoses (n = 16), the SEE was 16% for both the intra- and interobserver error, and for significant stenosis (n = 17), the SEE was 16% and 18% for the intra- and interobserver error, respectively. For oblique sagittal MPR measurements,

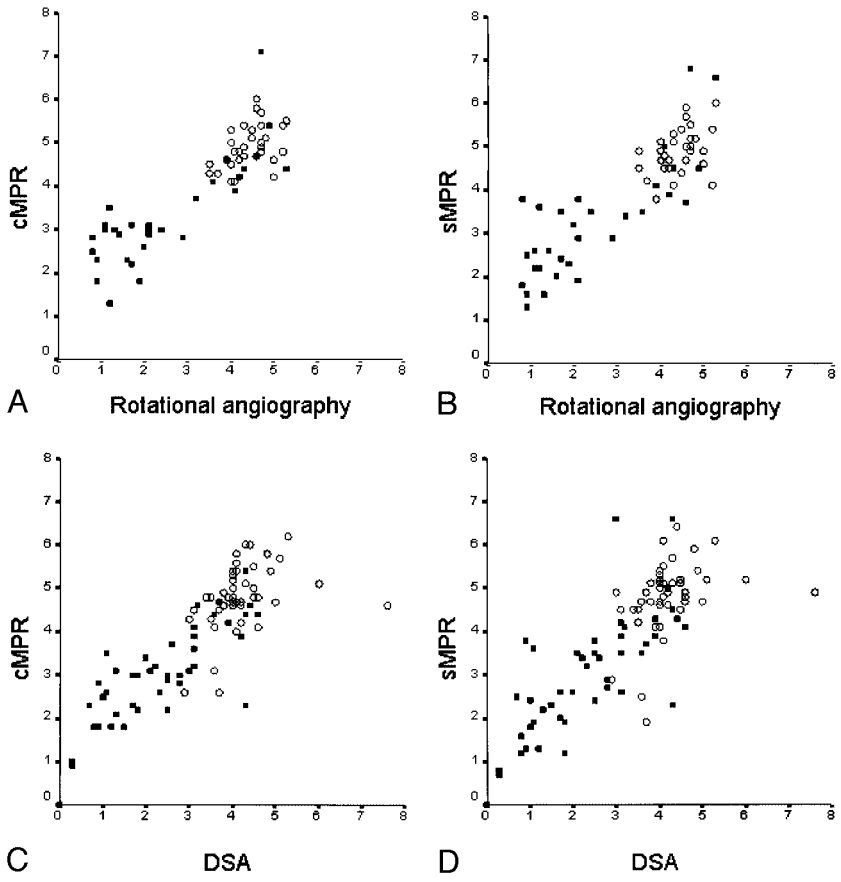

FIG 4. *A–D*, Scatterplots show the distribution of absolute diameters in millimeters between rotational angiography and cross-sectional MRP (*cMPR*) (*A*) and oblique sagittal MPR (*sMPR*) (*B*) of CT angiography and between DSA and cross-sectional MPR (*C*) and oblique sagittal MPR (*D*) of CT angiography. The absolute diameter measurements were obtained from the stenosed level (filled square) and from the reference level (open circle).

TABLE 2: CT Angiographic MPR measurements of degree of stenosis compared with rotational angiographic measurements in 33 carotid arteries

MPR Method	Observer	Mean Difference* (% ± SD)	*r* Value	κ Value (95% CI) 50%†	κ Value (95% CI) 70%‡
Cross-sectional	1	6.9 ± 17.6	0.82	0.58 (0.31–0.84)	0.40 (0.05–0.76)
	2	10.7 ± 16.1	0.86	0.58 (0.33–0.83)	0.29 (−0.04–0.62)
Sagittal	1	2.8 ± 19.2	0.80	0.70 (0.45–0.94)	0.40 (0.05–0.76)
	2	9.1 ± 16.8	0.84	0.58 (0.31–0.84)	0.42 (0.06–0.76)

* A positive mean difference value indicates an underestimation of stenosis degree with CT angiography.

† 50% cutoff point for hemodynamically significant stenosis.

‡ 70% cutoff point for hemodynamically significant stenosis.

the SEE was 24% and 25% for the intra- and interobserver error in insignificant stenoses, and 19% and 17% in significant stenoses, respectively.

Accuracy of CT Angiographic MPR Measurements

The Pearson correlation coefficient between CT angiography and rotational angiography measurements of the smallest diameter of the absolute residual lumen of carotid stenosis was 0.75 ($P < .001$) by using cross-sectional MPR and 0.66 ($P < .001$) by using oblique sagittal MPR for the first measurer, and the corresponding values for the second measurer were 0.84 ($P < .001$) and 0.83 ($P < .001$). The scatterplots of the absolute diameter measurements between rotational angiography or DSA and CT angiography in the stenosed carotid arteries are shown in Figure 4. The accuracy of CT angiography in the measurement of degree of stenosis in the carotid bifurcation area with reference to rotational angiography and DSA is shown in Tables 2 and 3, respectively.

Diagnostic Performance of Multi-Detector Row CT Angiography

Tables 4 and 5 show the diagnostic performance of CT angiography measurements in comparison with rotational angiography (n = 33) and DSA (n = 70), respectively. The combined MPR was considered to be positive when either the cross-sectional MPR or oblique sagittal MPR measurements yielded a degree of stenosis of 50% or greater. Simple visual estima-

TABLE 3: CT angiographic MPR measurements of degree of stenosis compared with DSA measurements in 70 carotid arteries

MPR Method	Observer	Mean Difference* (% ± SD)	*r* Value	κ Value (95% CI) 50%†	κ Value (95% CI) 70%‡
Cross-sectional	1	−0.4 ± 23.0	0.76	0.53 (0.33–0.73)	0.50 (0.27–0.72)
	2	5.3 ± 21.8	0.76	0.70 (0.53–0.87)	0.36 (0.14–0.58)
Sagittal	1	−3.8 ± 24.5	0.73	0.55 (0.36–0.74)	0.54 (0.32–0.76)
	2	3.7 ± 21.7	0.77	0.79 (0.65–0.94)	0.38 (0.15–0.61)

* A positive mean difference value indicates an underestimation of stenosis degree with CT angiography.

† 50% cutoff point for significant stenosis.

‡ 70% cutoff point for significant stenosis.

TABLE 4: Diagnostic performance of various CT angiographic MPR analysis methods for assessment of degree of stenosis in carotid arteries compared with rotational angiography

MPR Analysis Method	Observer	Sensitivity (%)	Specificity (%)	Overall Accuracy (%)
Cross-sectional	1	65 (11/17)	94 (15/16)	79 (26/33)
	2	59 (10/17)	94 (15/16)	76 (25/33)
Sagittal	1	82 (14/17)	88 (14/16)	85 (28/33)
	2	65 (11/17)	94 (15/16)	79 (26/33)
Combined*	1	82 (14/17)	88 (14/16)	85 (28/33)
	2	71 (12/17)	88 (14/16)	79 (26/33)

Note.—Numbers in parentheses are number of arteries. A 50% stenosis was the cutoff point for a hemodynamically significant finding.

* Combined MPR was considered to be positive when either of the MPR (cross-sectional or oblique sagittal) measurements yielded a positive result.

TABLE 5: Diagnostic performance of various CT angiographic MPR analysis methods for assessment of degree of stenosis in carotid arteries compared with DSA

MPR Analysis Method	Observer	Sensitivity (%)	Specificity (%)	Overall accuracy (%)
Cross-sectional	1	73 (22/30)	80 (32/40)	77 (54/70)
	2	77 (23/30)	98 (39/40)	88 (62/70)
Sagittal	1	87 (26/30)	70 (28/40)	77 (54/70)
	2	87 (26/30)	95 (38/40)	91 (65/70)
Combined*	1	87 (26/30)	70 (28/40)	77 (54/70)
	2	90 (27/30)	95 (38/40)	93 (66/70)

Note.—Numbers in parentheses are numbers of arteries. A 50% stenosis was the cutoff point for a hemodynamically significant finding.

* Combined MPR was considered to be positive when either of the MPR (cross-sectional or oblique sagittal) measurements yielded a positive result.

tion of the degree of stenosis yielded sensitivity of 100% (31/31), specificity of 73% (29/40), and overall accuracy of 86% (60/70) in comparison with DSA in our sample of 70 carotid arteries including both the symptomatic and contralateral sides.

On CT angiograms, two carotid arteries with the string sign indicating near occlusion were detected. One of these findings was the same as noted at DSA, and 95% stenosis was recorded by the first measurer. The other ICA with the string sign on CT angiograms was not interpreted to show the string sign at DSA, although a minor decrease in the diameter of the distal ICA could be seen. The degree of stenosis in this particular case was 90% at DSA.

An additional strategy was tested by using the highly sensitive visual estimation as the first-line screening step for detection of a hemodynamically significant stenosis (≥ 50%), and as the second step, the measurement of the degree of stenosis was applied only for the positive cases selected by visual estimation. In symptomatic sides (n = 35), the sensitivity of CT angiography was good with sufficient accuracy for detection of carotid stenosis (Table 6). The only false-positive case with CT angiography was a carotid bifurcation in which the stenosis degree was measured to be 43% at DSA, but 63% at rotational angiography.

CT angiography enabled detection of 14 ulcerative plaques in the 65 patent carotid arteries. In 11 cases, the finding agreed with those of DSA. Fourteen of the ulcerations diagnosed with DSA were not detected with CT angiography. Therefore, the agreement between CT angiography and DSA was 74% for detection of plaque ulceration.

All five occlusions in proximal ICAs verified with DSA were correctly diagnosed with CT angiography by all observers. In the remaining 66 patent ICAs, distal lesions were interpreted to be present in 13 cases (20%) with CT angiography. Four false-positive findings were due to the presence of extensive calcifications. Since there were no false-negative findings at CT angiography, we achieved a sensitivity of 100% (9/9), a specificity of 93% (53/57), and an overall accuracy of 95% (62/65) for detection of distal lesions

TABLE 6: Diagnostic performance of CT angiography in the assessment of carotid artery stenosis on the symptomatic side compared with DSA

Analysis Method of CT Angiography	Sensitivity (%)	Specificity (%)	Overall Accuracy (%)	PPV (%)	NPV (%)
Visual	100 (21/21)	50 (7/14)	80 (28/35)	75 (21/28)	100 (7/7)
Combined MPR*	95 (20/21)	86 (12/14)	91 (32/35)	91 (20/22)	92 (12/13)
Visual-quantitative†	95 (20/21)	93 (13/14)	94 (33/35)	95 (20/21)	93 (13/14)

Note.—PPV indicates positive predictive value; NPV, negative predictive value. Numbers in parentheses are number of arteries. A 50% stenosis was the cutoff point for a hemodynamically significant stenosis.

* Combined MPR was considered to be positive when either of the MPR (cross-sectional or oblique sagittal) measurements yielded a positive result.

† Visual-quantitative analysis consisted of first-line visual CT angiography interpretation and subsequent measurement only for the positive cases.

in the ICA. The one incidental middle cerebral artery aneurysm was correctly diagnosed with CT angiography. No adverse events were detected during the CT angiography, DSA, or rotational angiography procedures.

Discussion

Large randomized trials have shown that carotid endarterectomy is beneficial in the secondary prevention of stroke in symptomatic patients with high-grade stenosis (6–9). In the pooled data from these randomized controlled trials, some benefit was noted in those patients with 50–69% stenosis, whereas benefit in patients with near-occlusion of the carotid artery has been reported to be marginal in the short-term and uncertain in the long-term (7). Those trials used selective conventional angiography for the diagnosis and quantification of carotid stenosis.

Owing to the risks associated with angiography, alternatives such as the use of noninvasive carotid imaging have been proposed (10). Color Doppler sonography (11), MR angiography with or without contrast enhancement (12, 13), or CT angiography (14) has been proposed for the preoperative diagnosis of carotid stenosis, or possibly a combination of two noninvasive imaging methods (15).

The practice of using only noninvasive imaging for the assessment of carotid stenosis degree is not universally accepted (16–19), and it has been stated that proper validity assessment of noninvasive methods against conventional angiography within individual centers is required, including the risk of stroke due to angiography (7, 19). As long as there are no published reports from randomized studies based solely on noninvasive imaging methods, many institutions still perform carotid endarterectomy based on noninvasive imaging only in those cases where there are contraindications to angiography.

However, noninvasive imaging methods can be advocated for the screening of carotid artery disease to reduce the number of invasive angiographic procedures (i.e., only those patients with probable significant stenosis are subsequently selected for angiography).

Color Doppler sonography is a safe, relatively inexpensive and noninvasive method for detection of stenosis in the carotid artery. However, large variability exists in the performance of Doppler sonography to reliably assess hemodynamically significant carotid stenosis (20). Even though CT angiography has some disadvantages in comparison with other noninvasive imaging methods, such as exposure to ionizing radiation and use of potentially nephrotoxic contrast media, this technique has the potential to be used as a screening method for symptomatic patients with cerebrovascular disorders. The most common imaging technique for the primary diagnostics of hemispheric infarcts is CT of the brain. CT angiography could be easily performed in the same session for these patients at considerably lower cost compared with MR angiography, and without transfer of the patient to another imaging unit.

CT angiography provides several methods to display vascular structures. Axial source images and MPRs are the most informative images, containing all the information of the entire imaged volume, such as enhanced vascular structures, plaques in the arterial wall with or without mural calcifications, and extravascular tissues. However, a single axial image or MPR view displays only a substructure of an arterial tree. The interpretation of the complex vascular system necessitates viewing of several contiguous sections or views, and usually the interpretation of CT angiograms is performed interactively on a workstation (21). Three-dimensional reconstructions such as maximum intensity projection (MIP), shaded surface display (SSD), or volume rendering (VR) are able to display complex arterial anatomy and the findings in a single view. The interactive interpretation of CT angiograms in our daily practice includes scrolling of axial source images together with two MPR views in orthogonal directions (sagittal and coronal) to analyze vascular anatomy and pathologic conditions. If necessary, additional MPR views angled by the direction of the viewed vessel or curved reformations are obtained. The powerful computers of the workstation today allow easy generation of the 3D views; thus, for example, VR views are quickly available for the overview of the vascular anatomy and for demonstration of findings to the referring physician.

During the past decade, numerous studies showing good results on the diagnostic performance of single-section CT angiography to assess carotid stenosis have been published (22–32). For interpretation of CT angiograms, 3D views (SSD, MIP, or VR) have mainly been used. Mural calcification often hampered the depiction of the arterial lumen with a 3D

view alone, and therefore axial source images or MPRs were used in cases of calcified stenoses (23–26, 31, 33). In the study by Randoux et al (32), CT angiography with oblique MPR images had excellent correlation with DSA in terms of categories of stenosis, and the sensitivity and specificity of CT angiography reached 100% for detecting stenoses of 70% or more.

In a recent study, Alvarez-Linera et al (33) reported that contrast-enhanced MR angiography correlated better with conventional angiography than did CT angiography, but only 3D views (i.e., MIP and SSD) were used for the interpretation of CT angiography. However, the radiologist must be aware of the technical principles underlying those 3D reconstruction methods to avoid pitfalls in the evaluation of vascular lesions (1, 21, 34). Interpretation of CT angiography should always include analysis of the entire imaged volume interactively at the workstation by using axial images, MPRs, or both; probably, that might have increased the accuracy of CT angiography also in the above-mentioned study. When using interactive interpretation of axial sections, MPRs, and the 3D view, neither mural calcification nor enhanced jugular veins hamper the visualization of the carotid artery, and the carotid artery anatomy in relation to facial bones can also be displayed.

In the present study, we used the original 2D projectional data of rotational angiography as the reference for CT angiography diameter measurements. Irregular eccentric stenoses with noncircular lumen are common in carotid arteries. Therefore, the shortest diameter of the stenosed carotid segment is more likely to be revealed accurately with rotational angiography producing more projections than DSA. Our study showed that measurements from DSA tended to give slightly smaller degrees of stenosis than those of rotational angiography. In the five categories, rotational angiography and conventional DSA had considerable disagreement; however, this result is in line with that of the study by Elgersma et al (5).

The current study showed that, compared with rotational angiography, measurement of the carotid artery diameter with CT angiography by using MPR images was quite accurate in normal arteries and in mildly or moderately stenosed segments, but the accuracy decreased in cases of high-grade stenosis with a very small minimal diameter of the stenosed lumen. The scatterplots in Figure 4A and B show that the measurement of the diameter with CT angiography in moderately or severely stenosed carotid segments with a diameter less than 3 mm on rotational angiograms had the greatest error. When CT angiography measurements were compared with DSA measurements (Figs 4C and D and 5), that error was not as obvious, probably because of the inability of DSA to catch the view showing the shortest diameter in the stenosed carotid artery, which might compensate for the error in CT angiography measurements.

There was considerable variability between the observers in performing the measurements with CT angiography, and the intraobserver reproducibility was not high either, probably due to the inexperience of one of the observers in interpreting CT angiographic studies. Our study indicates that good experience of the radiologist interpreting CT angiographic studies is essential. The observers also had different methods for performing the MPR measurement, which enhanced the interobserver variability (Tables 2 and 3).

The intra- and interobserver error (SEE) was not decreased when comparing the category of significant carotid stenosis with insignificant stenosis. When using oblique sagittal MPR images, measurement of degree of stenosis was even more constant in the category of significant stenosis, whereas measurement of degree of stenosis from cross-sectional MPR views was on the same order for the two stenosis categories. Interpretation of the stenosis site might be easier and more constant when using cross-sectional images rather than sagittal images in cases of mild (insignificant) stenosis. In cases of high-grade stenosis, however, there is no difficulty in identifying where the maximal stenosis is regardless of the view used for the interpretation.

There are several possible reasons for the inaccurate determination of the diameter in the carotid artery with a high-grade stenosis. One reason may be the inability of the observer to place the digital calipers accurately in a stenosed artery with very small diameter, where the caliper almost hides the vessel (Fig 1A). Using magnification of the displayed image, some blurring of the structures occurs. In addition, in our CT angiography interpretation, we used wide window and level settings to visualize mural calcifications properly. The study by Liu et al (35) with a vessel phantom showed that the application of optimized window and level settings at CT angiography can reduce the measurement variability, because suboptimal window and level settings are the reason for edge blurring of the enhanced vessel; the smaller the actual luminal diameter, the greater the potential measurement error. This phenomenon may partly explain the failing of the CT angiography measurement to help accurately assess the diameter in cases of high-grade stenoses.

In another phantom study, by Suzuki et al (36), the reconstruction kernel for axial sections and insufficient attenuation of contrast medium have been proposed as possible sources of errors for assessment of the contrast column diameter with automated software. Movement of the pulsating carotid artery during CT angiography also may cause blurring of the vessel edges and even obscure a high-grade stenosis at CT angiography (Fig 6). However, if it is obvious that the measured stenosis degree is not reasonably precise, as evident in our study, there is no sense in basing the diagnosis only on a single measurement of the degree of carotid stenosis.

Conventional angiography is currently the only widely used reference method in clinical studies. In previous studies on the accuracy of CT angiography, DSA has been used as the reference. To be able to compare results with other studies for diagnostic accuracy of CT angiography, we also used DSA as a reference in that part of the study. In addition, rota-

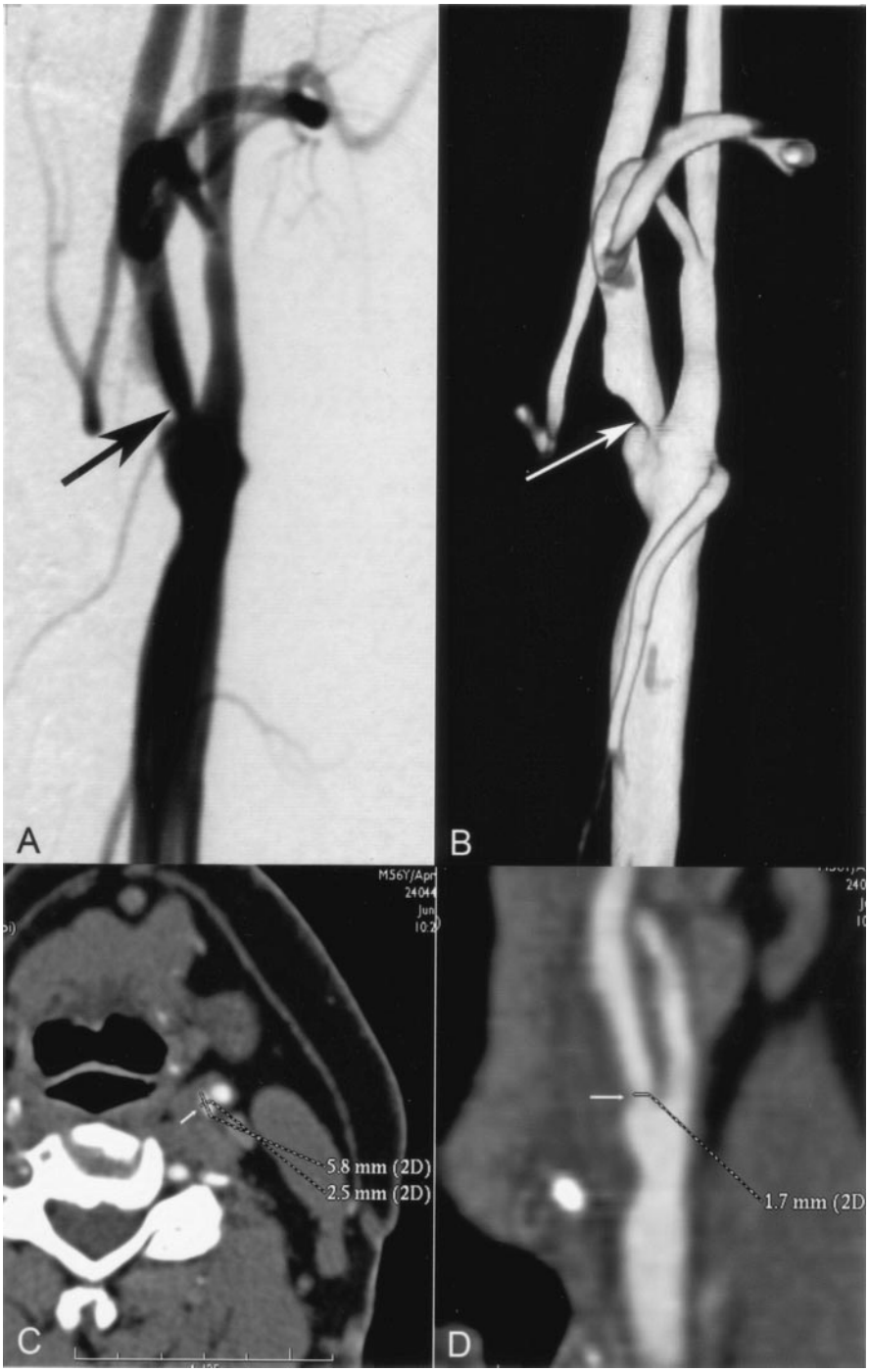

FIG 5. *A* and *B*, Selective angiogram of the left carotid artery (*A*) shows a stenosis in the proximal ICA (arrow), which was measured to be 58%. Three-dimensional rotational angiogram of the same carotid artery (*B*), which was reconstructed from the 80 original projections, shows the stenosis (arrow) without overlapping arterial branches. Note that only the original projection images (not shown) instead of 3D reconstructions were used in the study as the reference for CT angiography. The stenosis degree was measured to be 69% on the original rotational angiograms (not shown).

C and *D*, CT angiographic cross-sectional (*C*) and oblique sagittal (*D*) MPR images show no mural calcification at the maximum stenosis (arrow). White lines on the carotid artery indicate the manually measured diameters of the vessels. Cross-sectional MPR image (*C*) shows the noncircularity of the lumen at the stenosed level. With CT angiographic measurements by the two radiologists, the stenosis degree was underestimated by 28–38% on the cross-sectional MPR images compared with rotational angiographic measurements. The underestimation rate was lower (2–18%) with use of oblique sagittal MPR images. In this particular case, the stenosis degree was visually estimated to be 70% with CT angiography

tional angiography has not been used in large randomized studies as a standard, and in our study rotational angiography was not always performed on the symptomatic side, to avoid additional risks of angiography.

Although measurements of the absolute diameter with CT angiography were inaccurate compared with those of rotational angiography, especially in cases of high-grade stenosis, the diagnostic performance of CT angiography proved to be good in comparison with DSA (Table 5) when using a cutoff point of 50% or greater for the degree of hemodynamically significant stenosis, which is justified because some patients with a 50–69% stenosis in the carotid artery benefit from carotid endarterectomy (7).

During interpretation of CT angiography, it was obvious for the observers that the actual stenosis was often more severe than the numerical value of the MPR measurement (Fig 5). Perhaps further studies will give information on the optimal display of CT angiography to accurately measure the degree of carotid stenosis. Until then, however, we recommend that visual estimation of the stenosis be included for the diagnosis. In addition to the interpretation based on absolute diameter measurements, a third radiologist without knowledge of the measurements of the

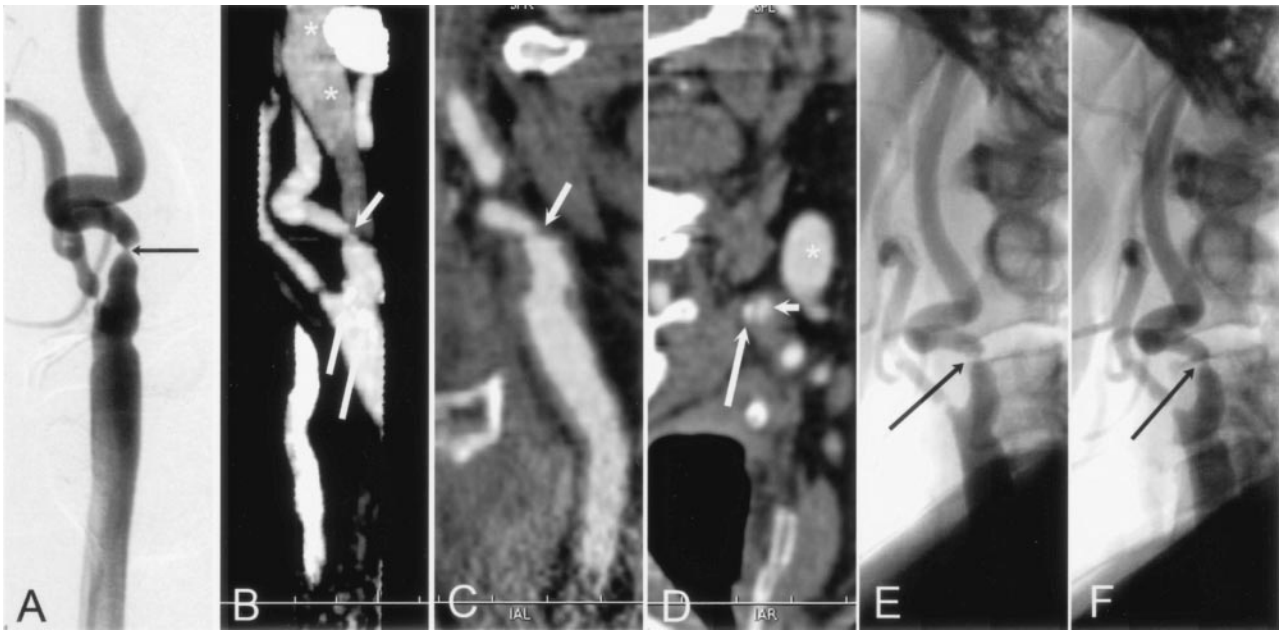

FIG 6. *A*, Right anterior oblique DSA image reveals high-grade stenosis (arrow) in the left ICA; degree of stenosis was calculated to be 82%. A high-grade stenosis is also present at the origin of the left external carotid artery.

B–D, CT angiograms verify the stenosis of the ICA (*short arrow*). Left sagittal view of 3D reconstruction MIP image (*B*) also shows stenosis of the external carotid artery. CT angiographic sagittal (*C*) and cross-sectional (*D*) MPR views reveal the stenosis in the ICA (short arrow) without over projection of mural calcification (long arrow). On the MIP image (*B*), mural calcification (*long arrows*) is over projected with the lumen. The degree of stenosis was considerably underestimated with CT angiography using the MPR measurements. However, the hemodynamic significance of the stenosis was obvious in the interactive interpretation of CT angiograms.

E and *F*, Rotational angiograms show that notable pulsation movement of the stenosed artery in the craniocaudal direction (arrow) can be detected when comparing the location of the stenosis to the upper endplate of the third cervical vertebra between these two images obtained in different phases of the cardiac cycle. The movement artifact might have caused extra blurring of the vessel wall on CT angiograms obtained without electrocardiographic gating.

two observers visually interpreted CT angiograms by using interactive interpretation of axial sections and MPR views for the diagnosis and simply estimated the degree of stenosis. Visual estimation proved to be the most sensitive method for identification of carotid stenosis of 50% or greater, but specificity was only modest. The combination of interactive interpretation of CT angiograms with subsequent MPR measurements for selected cases achieved the best diagnostic accuracy (Table 6).

In the present study, CT angiography for the symptomatic side showed sensitivity of 95%, specificity of 93%, and overall accuracy of 94%. The only false-positive case in CT angiography was possibly underestimated with DSA, because the degree of stenosis was significantly higher at rotational angiography. One false-negative case (Fig 6) was underestimated with MPR measurements but was nonetheless interpreted to be a significant stenosis in the interactive interpretation of CT angiography. In the study by Anderson et al (30), CT angiography with the interpretation of axial source images proved to be 89% sensitive, 91% specific, and 90% accurate in the detection of carotid stenosis greater than 50%. Our result is comparable to the result of that study, which was carried out with a single-detector device, but contrary to the study by Anderson et al, we did not have any unsuccessful CT angiographic studies to exclude from the analysis. The use of bolus tracking during the performance of CT angiography ensures sufficient attenuation of contrast medium in target vessels. In addition, the use of high-concentration contrast medium for CT angiography has been recommended (37). Before scanning, training the patient is also essential to reduce artifacts due to swallowing and moving.

For contrast-enhanced MR angiography, sensitivities as high as 100% for carotid stenosis have been reported, but spatial resolution remains poor for small vessels (38). CT angiography with the multidetector row technique has excellent spatial resolution also for smaller structures, but artifacts sometimes hamper the visualization of short stenoses (21). Our study was performed with a four-channel CT device. The capacity of newer multi-detector row CT devices with up to 64 sections per rotation is superior to the device used in our study. The 16-channel multidetector row CT device currently available for carotid imaging in our department produces images with fewer artifacts. In addition, the use of electrocardiographic gating developed for cardiac imaging significantly reduces movement artifacts in CT angiography; electrocardiographic gating can also be used for carotid arteries in cases with suspicion of tight stenoses. Alternatively, in ambiguous cases, the use of conventional angiography is advisable. Arguments for the use of conventional angiography for the confirmation of high-grade stenosis in symptomatic patients have also been proposed earlier to ensure appropriate treatment decisions (19).

Compared with subtracted contrast-enhanced MR angiography, CT angiography also demonstrates atherosclerotic changes inside the arterial wall with some morphologic characteristics of the plaque. Ulcerative plaques in carotid arteries may be the source of thromboembolism into the cerebral circulation (39). There was moderate agreement between the modalities for the detection of ulceration in the present study. Without proper verification of the plaque (pathoanatomic diagnosis), the true accuracy of each technique remains unknown. The accuracy of CT angiography for detection of carotid artery occlusion was high in our study, which is in agreement with that of previous studies (25, 30, 40).

The sensitivity of CT angiography in this study was excellent (100%) for the detection of distal lesions in the ICA. Other clinically relevant findings may also be revealed, such as intracranial aneurysms (41), which favors the use of CT angiography over Doppler sonography for noninvasive carotid imaging in symptomatic patients. Techniques enabling the removal of bone structures are under development (42), but according to our experience, evaluation of the ICA within the bone structures of the skull base with an interactive interpretation is sufficient for the purpose of diagnosis. The problem with CT angiography in intracranial stenoses is the prevalence of mural calcifications, manifesting sometimes as false-positive distal lesions in the ICA. Combining 3D time-of-flight MR angiography with CT angiography has been shown to improve the accuracy of the evaluation of intracranial steno-occlusive disease compared with the use of MR angiography alone (43).

There are some limitations in our study. The number of the patients is small, leading to a limited number of symptomatic carotid arteries, and some patients also had a normal carotid artery even on the symptomatic side. Further, there were few cases with distal carotid stenosis, leading to difficulties in interpretation of the results with regard to distal lesions. The window and level settings for interpretation of CT angiograms were selected empirically, but were selected so that the mural disruptive calcifications could be well differentiated from the enhanced vessel lumen (Fig 6). Actually, the proper window and level settings for the display of carotid stenosis with mural calcifications is still not known, although the use of a specifically adjusted narrow window setting has been proposed (21).

Commercial software is available for assessment of arterial stenosis. In our recent study, the reproducibility of commercially available automated 3D CT angiography analysis software proved to be good for assessment of carotid stenosis; however, this method requires the use of manual corrections in cases of interfering factors (44). In that ongoing study, we wanted to assess the manual method available for all CT users to measure carotid stenosis. In our current study, the measurement of diameters was performed only once without averaging of multiple measurements. That could be a limitation of the study, but usually in routine clinical work we seldom do multiple measurements. Interpretations of the studies also were performed in a clinical setting, sometimes leading to different interpretation of the stenosis site even between two different MPRs.

Conclusion

The result of the present study indicates that CT angiography with a single cross-sectional MPR or oblique sagittal MPR measurement of stenosis degree is not accurate enough to permit a clinical decision on further treatment in cases of high-grade stenosis. We recommend the use of the interactive interpretation of CT angiography to verify carotid stenosis, which sometimes reveals a hemodynamically significant carotid stenosis even though the measurement from either MPR image indicates insignificant stenosis ($< 50\%$).

CT angiography with the new multi-detector row technique was found to achieve good diagnostic accuracy in comparison with DSA. High sensitivity of CT angiography justifies the use of this method for screening of carotid stenosis in symptomatic patients. For significant stenoses revealed by CT angiographic screening, conventional angiography still seems to be necessary.

References

1. Rubin GD. **Techniques for performing multidetector-row computed tomographic angiography.** *Tech Vasc Interv Radiol* 2001;4:2–14
2. Rubin GD, Shiau MC, Schmidt AJ, et al. **Computed tomographic angiography: historical perspective and new state-of-the-art using multi-detector-row helical computed tomography.** *J Comput Assist Tomogr* 1999;23(suppl 1):S83–90
3. Tomandl BF, Klotz E, Handschu R, et al. **Comprehensive imaging of ischemic stroke with multisection CT.** *Radiographics* 2003;23:565–592
4. Bosanac Z, Miller RJ, Jain M. **Rotational digital subtraction carotid angiography: technique and comparison with static digital subtraction angiography.** *Clin Radiol* 1998;53:682–687
5. Elgersma OE, Buijs PC, Wust AF, van der Graaf Y, Eikelboom BC, Mali WP. **Maximum internal carotid arterial stenosis: assessment with rotational angiography versus conventional intraarterial digital subtraction angiography.** *Radiology* 1999;213:777–783
6. North American Symptomatic Carotid Endarterectomy Trial Collaborators. **Beneficial effect of carotid endarterectomy in symptomatic patients with high-grade carotid stenosis.** *N Engl J Med* 1991;325:445–453
7. Rothwell PM, Eliasziw M, Gutnikov SA, et al. **Analysis of pooled data from the randomised controlled trials of endarterectomy for symptomatic carotid stenosis.** *Lancet* 2003;361:107–116
8. Mayberg MR, Wilson SE, Yatsu F, et al. **Carotid endarterectomy and prevention of cerebral ischemia in symptomatic carotid stenosis. Veterans Affairs Cooperative Studies Program 309 Trialist Group.** *JAMA* 1991;266:3289–3294
9. European Carotid Surgery Trialists' Collaborative Group. **Randomised trial of endarterectomy for recently symptomatic carotid stenosis: final results of the MRC European Carotid Surgery Trial (ECST) [see comments].** *Lancet* 1998;351:1379–1387
10. Willinsky RA, Taylor SM, TerBrugge K, Farb RI, Tomlinson G, Montanera W. **Neurologic complications of cerebral angiography: prospective analysis of 2,899 procedures and review of the literature.** *Radiology* 2003;227:522–528
11. Calliada F, Verga L, Pozza S, Bottinelli O, Campani R. **Selection of patients for carotid endarterectomy: the role of ultrasound.** *J Comput Assist Tomogr* 1999;23(suppl 1):S75–81
12. Rofsky NM, Adelman MA. **Gadolinium-enhanced MR angiography of the carotid arteries: a small step, a giant leap? [editorial].** *Radiology* 1998;209:31–34
13. Remonda L, Senn P, Barth A, Arnold M, Lovblad KO, Schroth G. **Contrast-enhanced 3D MR angiography of the carotid artery: com-**

parison with conventional digital subtraction angiography. *AJNR Am J Neuroradiol* 2002;23:213–219
14. Moll R, Dinkel HP. **Value of CT angiography in the diagnosis of common carotid artery bifurcation disease: CT angiography versus digital subtraction angiography and color flow Doppler.** *Eur J Radiol* 2001;39:155–162
15. Patel MR, Kuntz KM, Klufas RA, et al. **Preoperative assessment of the carotid bifurcation: can magnetic resonance angiography and duplex ultrasonography replace contrast arteriography?** *Stroke* 1995;26:1753–1758
16. Masaryk TJ, Obuchowski NA. **Noninvasive carotid imaging: caveat emptor.** *Radiology* 1993;186:325–328
17. Barnett HJ, Broderick JP. **Carotid endarterectomy: another wake-up call.** *Neurology* 2000;55:746–747
18. Rothwell PM. **For severe carotid stenosis found on ultrasound, further arterial evaluation prior to carotid endarterectomy is unnecessary: the argument against.** *Stroke* 2003;34:1817–1819; discussion 1819
19. Derdeyn CP. **Catheter angiography is still necessary for the measurement of carotid stenosis.** *AJNR Am J Neuroradiol* 2003;24:1737–1738
20. Howard G, Baker WH, Chambless LE, Howard VJ, Jones AM, Toole JF. **An approach for the use of Doppler ultrasound as a screening tool for hemodynamically significant stenosis (despite heterogeneity of Doppler performance): a multicenter experience. Asymptomatic Carotid Atherosclerosis Study Investigators.** *Stroke* 1996;27:1951–1957
21. Prokop M, Engelke C. **Vascular system.** In: Prokop M, Galanski M, eds. *Spiral and Multislice Computed Tomography of the Body.* New York: Thieme; 2003:844–851
22. Dillon EH, van Leeuwen MS, Fernandez MA, Eikelboom BC, Mali WP. **CT angiography: application to the evaluation of carotid artery stenosis.** *Radiology* 1993;189:211–219
23. Marks MP, Napel S, Jordan JE, Enzmann DR. **Diagnosis of carotid artery disease: preliminary experience with maximum-intensity-projection spiral CT angiography.** *AJR Am J Roentgenol* 1993;160:1267–1271
24. Schwartz RB. **Neuroradiological applications of spiral CT.** *Semin Ultrasound CT MR* 1994;15:139–147
25. Leclerc X, Godefroy O, Pruvo JP, Leys D. **Computed tomographic angiography for the evaluation of carotid artery stenosis.** *Stroke* 1995;26:1577–1581
26. Papp Z, Patel M, Ashtari M, et al. **Carotid artery stenosis: optimization of CT angiography with a combination of shaded surface display and source images.** *AJNR Am J Neuroradiol* 1997;18:759–763
27. Leclerc X, Godefroy O, Lucas C, et al. **Internal carotid arterial stenosis: CT angiography with volume rendering.** *Radiology* 1999;210:673–682
28. Marcus CD, Ladam-Marcus VJ, Bigot JL, Clement C, Baehrel B, Menanteau BP. **Carotid arterial stenosis: evaluation at CT angiography with the volume-rendering technique.** *Radiology* 1999;211:775–780
29. Verhoek G, Costello P, Khoo EW, Wu R, Kat E, Fitridge RA. **Carotid bifurcation CT angiography: assessment of interactive volume rendering.** *J Comput Assist Tomogr* 1999;23:590–596
30. Anderson GB, Ashforth R, Steinke DE, Ferdinandy R, Findlay JM. **CT angiography for the detection and characterization of carotid artery bifurcation disease.** *Stroke* 2000;31:2168–2174
31. Binaghi S, Maeder P, Uske A, Meuwly JY, Devuyst G, Meuli RA. **Three-dimensional computed tomography angiography and magnetic resonance angiography of carotid bifurcation stenosis.** *Eur Neurol* 2001;46:25–34
32. Randoux B, Marro B, Koskas F, et al. **Carotid artery stenosis: prospective comparison of CT, three-dimensional gadolinium-enhanced MR, and conventional angiography.** *Radiology* 2001;220:179–185
33. Alvarez-Linera J, Benito-Leon J, Escribano J, Campollo J, Gesto R. **Prospective evaluation of carotid artery stenosis: elliptic centric contrast-enhanced MR angiography and spiral CT angiography compared with digital subtraction angiography.** *AJNR Am J Neuroradiol* 2003;24:1012–1019
34. Kirchgeorg MA, Prokop M. **Increasing spiral CT benefits with postprocessing applications.** *Eur J Radiol* 1998;28:39–54
35. Liu Y, Hopper KD, Mauger DT, Addis KA. **CT angiographic measurement of the carotid artery: optimizing visualization by manipulating window and level settings and contrast material attenuation.** *Radiology* 2000;217:494–500
36. Suzuki S, Furui S, Kaminaga T, Yamauchi T. **Measurement of vascular diameter in vitro by automated software for CT angiography: effects of inner diameter, density of contrast medium, and convolution kernel.** *AJR Am J Roentgenol* 2004;182:1313–1317
37. Fleischmann D. **Use of high concentration contrast media: principles and rationale—vascular district.** *Eur J Radiol* 2003;45(suppl 1):S88–93
38. Wutke R, Lang W, Fellner C, et al. **High-resolution, contrast-enhanced magnetic resonance angiography with elliptical centric k-space ordering of supra-aortic arteries compared with selective x-ray angiography.** *Stroke* 2002;33:1522–1529
39. McCarthy MJ, Loftus IM, Thompson MM, et al. **Angiogenesis and the atherosclerotic carotid plaque: an association between symptomatology and plaque morphology.** *J Vasc Surg* 1999;30:261–268
40. Chen CJ, Lee TH, Hsu HL, et al. **Multi-slice CT angiography in diagnosing total versus near occlusions of the internal carotid artery: comparison with catheter angiography.** *Stroke* 2004;35:83–85
41. Villablanca JP, Jahan R, Hooshi P, et al. **Detection and characterization of very small cerebral aneurysms by using 2D and 3D helical CT angiography.** *AJNR Am J Neuroradiol* 2002;23:1187–1198
42. Neuman J, Lin Z, Wu LB, et al. **Clinical evaluation of an automatic bone removal technique for improved CT angiography [lsqb]abstr[rsqb].** Presented at the 16th European Congress of Radiology, Vienna, Austria, March 7–11, 2003.
43. Hirai T, Korogi Y, Ono K, et al. **Prospective evaluation of suspected stenoocclusive disease of the intracranial artery: combined MR angiography and CT angiography compared with digital subtraction angiography.** *AJNR Am J Neuroradiol* 2002;23:93–101
44. Zhang Z, Berg MH, Ikonen AE, Vanninen RL, Manninen HI. **Carotid artery stenosis: reproducibility of automated 3D CT angiography analysis method.** *Eur Radiol* 2003;14:665–672